# *Curvatio*: low cost measurement system for spinal curvature

Martin Vincent Bloedorn[1], Daniel Ponce[2], Debora Soccal Schwertner[3], Arthur Santos[4] and Carlos Rodrigo de Mello Roesler[5]

***Abstract*— Good corporeal positioning provides various physiological benefits. For that reason, early diagnosis of postural deviations is key to a cost-effective and satisfactory treatment. This work initially analyses the current state of the art in spinal curvature assessment technologies, verifying that the majority of them is either expensive, invasive or poorly available – especially in developing countries. Based on this review, this work deploys a conception for a new measurement device through a sequential development methodology. This new conception for an accelerometer-based system is detailed and implemented using affordable and widely available components, achieving great cost reductions and ease of replication. The resulting prototype's measurements are validated through the use of an optical tracking system, and its performance is briefly discussed.**

## I. INTRODUCTION

A good corporeal positioning provides physiological benefits, keeps bodily functions and ranges of motion within satisfactory standards and preserves the autonomy of individuals [1]. For that reason, early diagnosis of postural deviations enables a more efficient, cost-effective and satisfactory treatment [2].To aid such diagnose, there are currently various methods, techniques and softwares designed to reliably assess corporal misalignments.As such, visual assessment based on a postural evaluation form — while still widely used — is being replaced by dedicated instruments that quantify deviations, because observational procedures yield only qualitative and subjective data [3], with low inter-evaluator reliability [4].

Radiological examination (X-ray) has been considered the gold standard in measuring curvatures of the vertebral column [5]. However, it poses health risks due to the usage of ionizing radiation, classified as cancerous [6]. Furthermore, there may be measurement errors associated with evaluators' subjectivity [7].

Non-invasive body surface's contour evaluation systems are being developed to reduce health hazards. Scanning equipments and Magnetic Resonance Imaging (MRI) yield precise data [8, 9], but are expensive, require the patient to remain still throughout the measuring procedure [10] and do not allow the measurement of Range of Motion (ROM) in real time.

Photogrammetry requires methodological rigor to hinder measurement errors [11], and its not available for everyday measurements in regular clinics [11].

Accelerometers are being effectively employed to assess the spinal kinematics, in particular, the posture and ROM of the spinal segments. These devices register distances and tilt variations in relation to a plumb line. Such an equipment — shaped as a computer mouse (*SpinalMouse*®) — while being driven along the vertebral column's median line, sends displacement and tilt information to a computer. The data is collected in 1.3*mm* intervals, which yields a sampling rate of approximately 150Hz [12]. This equipment has been shown valid and reliable [13].

This accelerometer-based system essentially works as a precise goniometer, providing quick response times and easy handling. However, the said device is relatively costly, and hardly affordable in the developing world - especially in hospitals or clinics supported exclusively by public health systems. Furthermore, its measurement protocol and software renders the system incapable of assessing cervical curvatures.

With this analysis in mind, the present study describes the design and validation of a non-invasive, accelerometer-based device for postural assessment, that employs a similar operating principle as the aforesaid *SpinalMouse*®, while attempting to overcome its main disadvantages — high cost and low availability.

## II. MATERIALS AND METHODS

Based on the problematic above mentioned, a novel accelerometer-based measuring system conception is proposed. This conception was sequentially deployed by a systematic design methodology including the implementation and validation of a prototype.

### A. Design of the new measuring system

The sequential development of the new conception is inspired on [14] and consists of four phases: Planning design, Informational Design, Conceptual Design and Preliminary Design. For the sake of succinctness, a throughout detailing of each phase will not be provided. Instead, they will be briefly addressed in the following.

Initially, at the Planning Design phase, the objective of the design is defined. Considering the exposed problem,

[1]Martin Vincent Bloedorn is with the Department of Systems and Automation, Federal University of Santa Catarina (UFSC), 88040-900 SC Florianpolis, Brazil martin.bloedorn@gmail.com

[2]Daniel Ponce is with the Department of Mechanical Engineering, Federal University of Santa Catarina (UFSC), 89065-300 SC Blumenau, Brazil daniel.alejandro@ufsc.br

[3]Debora Soccal Schwertner is with the State University of Santa Catarina (UDESC), 88035-901 SC Florianpolis, Brazil debora.soccal@udesc.br

[4]Arthur Santos is with the Department of Mechanical Engineering, Federal University of Santa Catarina (UFSC), 88040-900 SC Florianpolis, Brazil arthur.pgsantos@gmail.com

[5]Carlos Rodrigo de Mello Roesler is with the Department of Mechanical Engineering, Federal University of Santa Catarina (UFSC), 88040-900 SC Florianpolis, Brazil rroesler@hu.ufsc.br

TABLE I

MAIN DESIGN SPECIFICATIONS FOR DEVELOPMENT OF A NEW MEASURING SYSTEM CONCEPTION.

| Specification list | Target values |
|---|---|
| 1. Acquire position | Dynamic range: 0-1500mm; Resolution: 2mm |
| 2. Acquire angular position | Dynamic range: 0-360°; Resolution: 1° |
| 3. Inexpensive | Demand |
| 4. Including cervical assess | Demand |
| 5. Real time curvature visualization | Demand |

the development of an accelerometer-based system for the assessment of spinal kinematics is proposed.

At the Informational Design phase the design specifications are identified and arranged according to its priority. In order to illustrate it, the main design specifications are shown in the left column of the Table I. In the right column are the target values: they consists of magnitudes or demands that must be accomplished.

The Conceptual Design phase yields a conception of a new measuring system. This conception is obtained by a choice of different components that fulfill the design specifications. The best chosen conception will be explained as a function of its selected components, shown in the Signal Flow diagram in Figure 1.

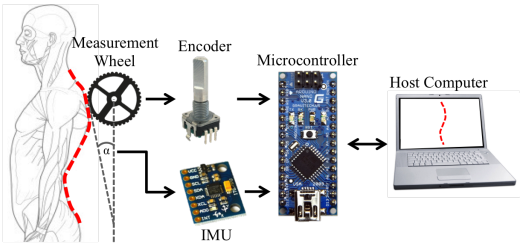


Fig. 1. Signal flows between components in the proposed system.

As shown, the prototype employs a *Measurement wheel* that contacts the surface whose curvature is to be measured. This wheel applies torque to a rotary Encoder (*Bourns*® PEC11R), which outputs a pulsed signal at each specified fraction of a turn. As the prototype is moved along the measured surface, its orientation changes are measured by an Inertial Measurement Unit (IMU, *Invensense*® MPU6050). The IMU and Encoder signals are processed by an embedded Microcontroller (*Arduino*® Nano), which relays this information to a Host Computer. The measured curvature is then displayed in a 3D representation. All the aforementioned components were chosen due to their broad availability and low-cost (prices range from 5 USD to 35 USD).

## B. Hardware

Following the methodology, the Preliminary Design phase was then initiated. Using a Computed-Aided Design (CAD) tool, an enclosure was designed to properly house the system's components presented in Figure 1. Also, a *measurement wheel* and a secondary *support* wheel were designed.

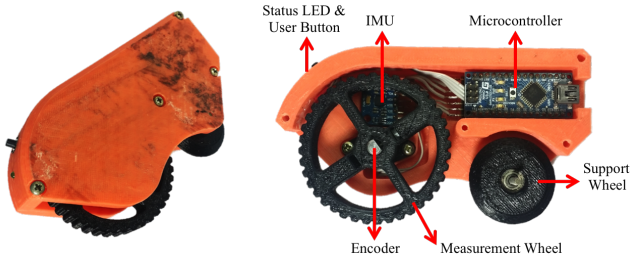


Fig. 2. **Left)** Finished assembled prototype. **Right)** Lateral view of the prototype, with components exposed and highlighted.

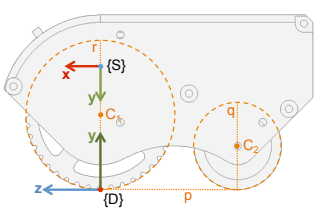


Fig. 3. Frames of reference attached to the prototype. The $z$-axis of $\{D\}$ is collinear to line segment $p$, which is tangent to the *Measurement* and *Support* wheels. The $y$-axis of $\{D\}$ points towards the *Measurement wheel's* center of rotation, $C_1$.

These parts were then fabricated with a 3D printer, using conventional *Acrylonitrile butadiene styrene* (ABS) plastic. The assembled prototype and the arrangement of its components can be seen in Figure 2.

The *measurement wheel* was designed with 60*mm* in diameter. It is attached directly to the chosen *encoder*, which outputs 96 transitions (pulse edges) per rotation. Together, the pair yields a measurement resolution of 1.9635*mm*, in conformity with the design specifications. A freely-rotating *secondary wheel* provides a second contact point during measurements.

The IMU is housed parallel to the *measurement wheel*. In such configuration, the IMU's frame of reference $\{S\}$ (as informed in [15]), has its axes parallel to the device's frame of reference $\{D\}$: $D_x \parallel S_z$, $D_y \parallel S_y$ and $D_z \parallel S_x$. The configuration is visible in Figure 3.

The assembled prototype is compact (123*mm* long, 70*mm* wide and 33*mm* thick) and light (82*g*), enabling easy manipulation. Measurements are thus realized by moving the prototype along a surface/object, with both wheels simultaneously contacting it. Vertebral curvature measurements are realized by driving the device along the median line groove on the patient's back.

## C. Software

The microcontroller in the measurement device streams orientation and odometry data to a host computer over an USB link. Through the use of external software interrupts, encoder transitions can reliably measured up to approximately 90kHz. Direction of the *measurement wheel's* rotation is also detected.

Furthermore, the microcontroller resorts to an *Inter-Integrated Circuit* ($I^2C$) bus to read data off the IMU at 50Hz.

The IMU embeds a three-axes accelerometer and a three-axes gyroscope, and yields the raw data of their readings. This data is then fused using a complementary filter which is shown to have results similar to the better-known Kalman filter [16], though requiring less computational power and enabling easier implementation.

In this application, the goal is to estimate the roll and pitch angles ($\theta$ and $\psi$, respectively) of the device's reference frame $\{D\}$, in relation to the direction of gravity. Thus, yaw measurements are disregarded. Let $a_{j,k}$ be the $k$-th raw accelerometer sample from axis $j$, and $g_{i,k}$ the raw angular velocity around axis $j$ ($j$ being either $x$, $y$ or $z$ of $\{S\}$). Initially, roll and pitch angle estimations are calculated based only on the accelerometer's data (${}^a\theta$ and ${}^a\psi$). Due to the relationship between the $\{S\}$ and $\{D\}$ reference frames stated before, we can write

$$ {}^a\theta_k = \text{atan}\left(\frac{a_{z,k}}{\sqrt{a_{x,k}^2 + a_{y,k}^2}}\right) \quad {}^a\psi_k = \text{atan}\left(\frac{a_{y,k}}{\sqrt{a_{x,k}^2 + a_{z,k}^2}}\right) \tag{1} $$

In the digital implementation, the standard four-quadrant inverse tangent function `atan2(Y,X)` is used. This function returns values in the closed interval $[-\pi, \pi]$ and can deal with zero-valued input arguments. In the following, the angular velocity measured by the gyroscope is numerically integrated via the trapezoidal rule,

$$ {}^g\Delta\theta_k = \frac{(K_y g_{y,k} + {}^g\Delta\theta_{k-1})}{2}\Delta t \quad {}^g\Delta\psi_k = \frac{(K_z g_{z,k} + {}^g\Delta\psi_{k-1})}{2}\Delta t \tag{2} $$

where ${}^g\Delta\theta_k$ and ${}^g\Delta\psi_k$ are pitch and roll angle changes as measured by the gyroscope during $\Delta t = t_k - t_{k-1}$, the time interval between two successive measurements. $K_y$ and $K_z$ are constant values, converting the IMU's raw readings to $rad/s$ values. Lastly, the complementary filter is computed,

$$ \begin{aligned} \theta_k &= \alpha(\theta_{k-1} + {}^g\Delta\theta_k) + (1-\alpha)({}^a\theta_k) \\ \psi_k &= \alpha(\psi_{k-1} + {}^g\Delta\psi_k) + (1-\alpha)({}^a\psi_k) \end{aligned} \tag{3} $$

where $0 \leq \alpha \leq 1$ was experimentally chosen at 0.97.

The application on the host computer then receives the orientation and odometry data from the measurement device, reconstructs the trajectory it followed and draws it in real-time on the screen. This trajectory stitching process assumes that the $y$-axis of $\{D\}$ is normal to the current segment being measured, and that the motion of the measurement device occurs predominately along the $z$-axis of $\{D\}$.

Let $\theta_k$, $\psi_k$ be the roll and pitch angles and $d_k$ be the incremental count of encoder transitions. The $k$-th point $\mathbf{p}$ in the stitched trajectory is given by

$$ \mathbf{p}_k = \mathbf{p}_{k-1} + R_y(\theta_k) R_x(\psi_k) K_d \begin{bmatrix} 0 \\ 0 \\ d_k - d_{k-1} \end{bmatrix} \tag{4} $$

where $R_y(\theta_k)$ and $R_x(\psi_k)$ are rotation matrices around the $Y$ and $X$ axes, and $K_d = 1.9635$ is a constant conversion between the number of encoder transitions and milliliters.

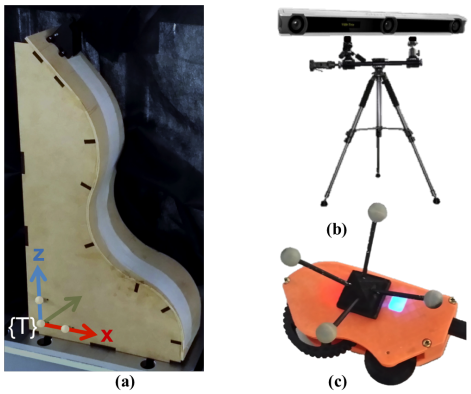


Fig. 4. Elements used in the validation setup. **(a)** Wooden template. Three tracking markers mounted onto it are used to define the $\{T\}$ coordinate system, with axes parallel to the template's outer edges. **(b)** *Optitrack*® camera used for measurement referencing. **(c)** Prototype fitted with tracking markers.

For $k = 0$, $\mathbf{p}_k$ sits at the measurement's origin, so that $\mathbf{p}_0 = \begin{bmatrix} 0 & 0 & 0 \end{bmatrix}^T$.

## III. VALIDATION

To validate the functionality of the designed system, its measurements and reconstructed trajectory were compared against an optical tracking system (*Optitrack® V120 Trio*), capable of tracking special markers with a $0.1mm$. A wooden profile was designed and assembled to serve as a measurement template. Three reflective markers mounted on this template define its reference frame $\{T\}$. The prototype was also fitted with reflective markers. All elements of this setup are depicted in Figure 4.

During validation measurements, the prototype was driven along the template, from top to bottom, in a slight diagonal from right to left. A 3D printed support mounted at the top of the template provides repeatable initial positioning across measurements. 30 successive measurements were performed by the same operator.

## IV. RESULTS

For each validation measurement executed, the reconstructed trajectory was first graphically compared to the measurements of the optical tracking system (here considered as the reference). One such plots is presented in Figure IV: data is presented in the measurement template's reference frame $\{T\}$ , in both the sagittal and coronal planes. The average errors over the 30 measurements are presented in table II (all units are in *mm*).

TABLE II
VALIDATION RESULTS. ALL UNITS ARE IN *mm*.

| Error | Mean | RMSE |
|---|---|---|
| Sagittal plane | 4.5 | 27.5 |
| Coronal plane | 3.9 | 25.1 |

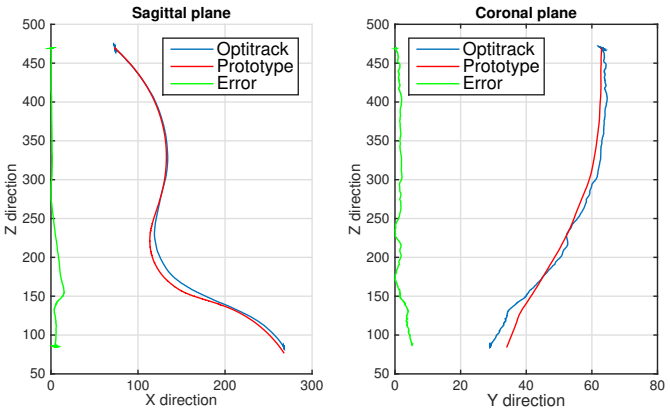


Fig. 5. Visualization of one of the validation measurements, in both the sagittal and coronal planes. The blue line represents the reference data obtained with the optical tracking device. The red line is the prototype's reconstructed trajectory. All data is represented in the reference frame $\{T\}$. All units are in *mm*.

## V. CONCLUSIONS AND FUTURE WORKS

The results shown in section IV present a slight drift between the prototype's data and the reference measurements, but are nonetheless promising. The overall shapes of the plotted data are very similar, and the RMSE between datasets in all validation measurements did not exceed 28*mm*. This results can be further improved by improving the prototype's calibration and software. Furthermore, the prototype's hardware and software has much room for improvement.

Finally, specifications posed in Table I were predominately satisfied. As presented in section II-B, the chosen *encoder* plus the designed *measurement wheel* yield a measurement resolution below the 2*mm* target value of specification #1. Validation measurements were performed over an average of 600*mm*, so the required dynamic range remains to be entirely assessed. The chosen IMU combined with the software implementation fulfill requirement #2. Specification #3 demanded inexpensiveness: the prototype can be fully assembled and programmed with less than 100 USD in material costs. This represents a cost reduction of over 40 times compared to similar products on the market. As-is, the prototype can also fulfill requirement #4 — but a more detailed protocol for such must be elaborated. Lastly, the system is capable of drawing the measured curvature in real time on a host computer, satisfying specification #5. Real-time ROM evaluation can also be performed.

## REFERENCES


[1] F. Mourey, C. A., and P. P., "Posture and aging. current fundamental studies and management concepts," *Presse Md*, 2000.

[2] B. Krawczky, A. G. Pacheco, and M. R. M. Mainenti, "A systematic review of the angular values obtained by computerized photogrammetry in sagittal plane: A proposal for reference values," *Journal of Manipulative and Physiological Therapeutics Computerized Photogrammetry*, 2014.

[3] P. Conti, E. Sakano, M. d. O. Ribeiro, C. Schivinski, and J. Ribeiro, "Assessment of the body posture of mouth-breathing children and adolescents," *Jornal de Pediatria*, 2011.

[4] D. Iunes, D. Bevilaqua-Grossi, A. Oliveira, F. Castro, and H. Salgado, "Comparative analysis between visual and computerized photogrammetry postural assessment," *Rev Bras Fisioter*, 2009.

[5] P. Hahn, C. Ulguim, and A. Badara, "Estudo retrospectivo das curvaturas da coluna vertebral e do posicionamento pelvico em imagens radiograficas," *Sade*, 2011.

[6] C. Roobottom, G. Mitchell, and G. Morgan-Hughes, "Radiation- reduction strategies in cardiac computed tomographic angiography," *Clin. Radiol.*, 2010.

[7] P. Roussouly and J. Pinheiro-Franco, "Sagittal parameters of the spine: Biomechanical approach," *Eur Spine J*, 2011.

[8] L. Tomkinson, R. Grant, and G. Shaw, "Quantification of the postural and technical errors in asymptomatic adults using direct 3d whole body scan measurements of standing posture," *Gait and Posture*, 2013.

[9] S. Cargill, M. Pearcy, and M. Barry, "Three-dimensional lumbar spine postures measured by magnetic resonance imaging reconstruction," *Spine*, 2007.

[10] H. Dannen and G. Water, "Whole body scanners," *Displays*, 1998.

[11] C. Fortin, D. Feldman, F. Cheriet, and H. Labelle, "Clinical methods for quantifying body segment posture: A literature review," *Spine*, 2011.

[12] A. Mannion, K. Knecht, G. Balaban, and J. Dvorak, "A new skin-surface device for measuring the curvature and global and segmental ranges of motion of the spine: Reliability of measurements and comparison with data reviewed from the literature," *Eur Spine J.*, 2004.

[13] A. Topalidou, G. Tzagarakis, X. Souvatzis, G. Kontakis, and P. Katonis, "Evaluation of the reliability of a new non-invasive method for assessing the functionality and mobility of the spine," *Acta of Bioengineering and Biomechanics*, 2014.

[14] G. Pahl and W. Beitz, *Engineering design: A systematic approach*. Springer Science & Business Media, 2013.

[15] *Mpu-6000 and mpu-6050 product specification*, MPU6050, Rev. 3.4, InvenSense Inc., Aug. 2013.

[16] W. T. Higgins, "A comparison of Complementary and Kalman Filtering," *IEEE Trans. Aerospace and Electronic Systems*, 1975.